Article

Emission Laws and Influence Factors of Greenhouse Gases in Saline-Alkali Paddy Fields

Jie Tang [1,2], Shuang Liang [1,2], Zhaoyang Li [1,2,*], Hao Zhang [1,2], Sining Wang [1,2] and Nan Zhang [3]

[1] Key Lab of Groundwater Resources and Environment, Ministry of Education, Jilin University, Changchun 130021, China; tangjie@jlu.edu.cn (J.T.); liangshuang13@mails.jlu.edu.cn (S.L.); zhao14@mails.jlu.edu.cn (H.Z.); snwang14@mails.jlu.edu.cn (S.W.)
[2] College of Environment and Resources, Jilin University, Changchun 130021, China
[3] Engineering College of Jilin University, Changchun 130026, China; zhangnan68@jlu.edu.cn
[*] Correspondence: zhaoyang@jlu.edu.cn; Tel.: +86-186-8665-1027; Fax: +86-431-8515-9440

Abstract: The study of greenhouse gas emissions has become a global focus, but few studies have considered saline-alkali paddy fields. Gas samples and saline-alkali soil samples were collected during the green, tillering, booting, heading and grain filling stages. The emission fluxes of CO_2, CH_4, and N_2O as well as the pH, soil soluble salt, available nitrogen, and soil organic carbon contents were detected to reveal the greenhouse gas (GHG) emission laws and influence factors in saline-alkali paddy fields. Overall, GHG emissions of paddy soil during the growing season increased, then decreased, and then increased again and peaked at booting stage. The emission fluxes of CO_2 and CH_4 were observed as having two peaks and a single peak, respectively. Both the total amount of GHG emission and its different components of CO_2, CH_4, and N_2O increased with the increasing reclamation period of paddy fields. A positive correlation was found between the respective emission fluxes of CO_2, CH_4, and N_2O and the available nitrogen and SOC, whereas a negative correlation was revealed between the fluxes of CO_2, CH_4, and N_2O and soil pH and soil conductivity. The study is beneficial to assessing the impact of paddy reclamation on regional greenhouse gas emissions and is relevant to illustrating the mechanisms concerning the carbon cycle in paddy soils.

Keywords: greenhouse gas; emission law; pH; soil soluble salt; available nitrogen; soil organic carbon; saline-alkali paddy fields; reclaimation period

1. Introduction

The Intergovernmental Panel on Climate Change (IPCC) Third Assessment Report (2001) forecasted that the global average temperature could rise from 1.4 °C to 5.8 °C from 1990 to 2100. Such changes are expected to have a great impact on the ecosystems of the Earth (*i.e.*, rising sea levels, changes in biome distribution and food production, and increased morbidity and mortality rates). Consequently, the study of greenhouse gas (GHG) emissions has become a global focus. Carbon dioxide (CO_2), methane (CH_4), and nitrous oxide (N_2O) are dominant greenhouse gases which contribute to about 60%, 20%, and 6% of the global warming potential, respectively [1]. Agricultural production is an important human activity, and paddy soil plays an important role in carbon sequestration [2,3]. However, rice plants release a certain amount of GHGs in the growing season [4,5]. Hence, the overall contribution of paddy ecosystems to global climate change needs to be explored. Microbes can decompose soil organic matter of farmlands into inorganic carbon and nitrogen. Inorganic carbon is released into the atmosphere as CO_2 under aerobic conditions, whereas it is released as CH_4 under anaerobic conditions [6,7]. Ammonium nitrification can be converted into nitrate nitrogen by nitrifying

bacteria, and nitrate nitrogen can be converted into nitrogen oxides in various forms by denitrifying bacteria. Therefore, N_2O is produced by nitrification and denitrification.

GHG emissions have been studied in various ecosystems, such as dryland, grassland, wetland, forest and paddy fields [8–12], and rice production is one of the largest emission sources of agriculture [13]. China is one of the most important rice-producing countries in the world. In China, the areas dedicated to rice harvests (3.2×10^7 ha) account for 22% of the world's total area (14.3×10^7 ha), and rice production in the country accounts for 38% of the total global yield [14]. Thus far, massive efforts have been made to quantify the GHG emissions of paddy fields in China, such as the study of winter paddy fields in hilly areas of Southwest China and wetlands in Sanjiang Plain of northeast China [15–17]. However, few studies have considered saline-alkali paddy fields which are rich in carbonate. The intense soil salinity and alkalinity could reduce biological performance [18] and significantly influence plant growth [19], subsequently affecting the soil carbon cycle process. Western Jilin Province, located in the southwest of Songnen Plain in China, is one of the three regions with the largest areas of concentrated distribution of saline-alkali soil worldwide. It is a sensitive area for climate change and is critical for carbon cycle studies. Significant climate change in the area has been recorded since the 1960s. The average temperature rose at a rate of 0.3 $^{\circ}C \cdot 10$ years^{-1}, the precipitation reduced at a rate of 1.0 mm$\cdot 10$ years^{-1} and snow cover days decreased at a rate of 3.8 day$\cdot 10$ years^{-1}; drought frequency continued to increase as well. The dry and warm climate worsened land salinization [20]. Large-scale reclamation of paddy fields began in the 1950s, forming an irrigation area of western Jilin Province. Moreover, the paddy field reclamation and food production programs implemented by the government of Jilin Province in 2009 further changed the land use patterns and GHG emissions in the area. A large amount of water from irrigation channels or underground is diverted at the beginning of the reclamation of saline-alkali land, then flows away with soluble salt. Irrigation and drainage are repeated over many years, until the paddy soil becomes rich enough, an estimation made by the local farmers based on the growing situation and yield of rice. The growing stages of rice include green, tillering, booting, heading, and grain filling stages. The nutrient absorbed by the rice and the carbon fixed by photosynthesis are mainly used for the growth of plants and roots from the green to heading stage, and those are stored in the fruits until the grain filling stage. The distribution of the rice-assimilated C into soil organic matter becomes slower and smaller with advances in the rice growing stage, and the percentage of rice-assimilated C emitted as CH_4 at the tillering, booting, and grain filling stages is 0.003%, 0.26%, and 0.30%, respectively [21]. Previous studies have indicated that remarkable changes of GHG emissions have been observed in different growing stages [22,23]. Thus, it is necessary to measure GHG emissions during the entire growing season. The saline-alkali paddy fields in western Jilin Province are taken as the research object of this paper. GHGs emission laws and influence factors of paddy fields are observed through field sampling. The study results provide scientific bases for the further assessment of the impact of paddy reclamation on global warming. The results can also serve as reference for future explorations into carbon cycle mechanisms on a regional scale.

2. Materials and Methods

2.1. Study Area Description

Western Jilin Province in northeast China is located at the eastern edge of Kerqin grassland and is located at 123°09′ E–124°22′ E, 44°57′ N–45°46′ N. Baicheng City, Songyuan City, and 10 counties are located in this area, which has a population of 4.73 million within a total area of 47,000 km^2 [24]. The area belongs to the farming-pastoral ecotone, and is a sensitive area for climate change. The area is an important agricultural and livestock production base and is considered one of the world's largest soda saline-alkali areas. The climate of the area is a typical semi-arid and semi-humid monsoon with four distinct seasons. The annual average rainfall, evaporation, and temperature are approximately 400 mm, 1700 mm and 4 $^{\circ}C$, respectively. The study area is part of a huge Meso-Cenozoic Songliao

fault basin. Its landform is generally like a dustpan in the east, while its south and west areas are comparatively higher than the north. The main rivers of the surface drainage are the Nen, Songhua and Er'songhua Rivers, and the tributary rivers include the Tao'er and Lalin Rivers. The flow of the rivers has been reduced owing to surface water development [24].

2.2. Soil Sampling and Test

The large-scale paddy reclamation program of the Mongolian Autonomous County of Qian Gorlos (Qianguo County) began in the 1950s, leading to the sizeable Qianguo irrigation. The Jilin Provincial Government has recently channeled the waters of Nen River to irrigate salinized land, further reclaiming paddy fields. The reclamation of paddy fields in Qianguo, which was the typical irrigation area in western Jilin Province, was determined according to soil type and land utilization type maps based on the remote sensing interpretation data generated by the Landsat MSS/TM images and field surveys. The fields are saline-alkali lands without vegetation before reclamation, and rice is cultivated for one growing season in the fields every year after reclamation. Paddy fields in western Jilin Province were steeped in early May and transplanted on 26 May 2012 (*i.e.*, the rice variety used was Tonghe 838). The water depths of the paddy fields ranged from 3 cm to 4 cm in the green stage, 1 cm in the early tillering stage, and 3 cm in the late tillering and booting stage. The fields are alternating wet and dry in the heading stage. Base fertilizer was applied prior to seeding, green and tillering fertilizer was applied after transplanting, and booting fertilizer was applied in early and late July. The annual fertilizer application rate was 150 kg$\cdot$N$\cdot$ha^{-1}. During the green, tillering, booting, heading, and grain filling stages in the year 2012, 0 cm to 30 cm surface soil samples from paddy fields of 1, 5, 15, 25, 35, and 55 reclamation years (Table 1) were respectively collected using the multi-point snakelike method. The samples were taken back to the lab for testing.

Table 1. The location of the sample points and the basic physicochemical properties of the soil.

Tillage History/year	Latitude	Longitude	Bulk Density (g$\cdot$cm^{-3})	SOC (g$\cdot$kg^{-1})	Total N (g$\cdot$kg^{-1})	Total P (g$\cdot$kg^{-1})
1	124.11625°	45.42197°	1.32	4.29	0.78	0.57
5	124.70649°	45.01740°	1.29	11.11	1.25	0.72
15	124.76833°	45.04847°	1.28	15.26	1.56	0.85
25	124.71742°	45.00526°	1.29	16.98	1.78	0.88
35	124.71202°	45.00006°	1.27	20.12	2.02	1.02
55	124.68689°	45.00671°	1.26	23.06	2.24	1.14

Soil samples were air-dried, crushed, and sieved through 2 mm, 1 mm, and 0.149 mm mesh. Soil organic carbon (SOC) was determined by using the SSM-5000A module of total organic carbon (TOC) analyzer (Shimadzu TOC-V, Japan). The pressure and flow of carrier gas were 200 Kpa and 500 mL$\cdot$min^{-1}, respectively. Duplicate homogenized soil samples sieved through a 0.149 mm mesh were separately placed into TC and IC samples boats, and burned at 900 °C with catalyst and at 200 °C after acidified with analytically pure phosphoric acid, respectively. Then, the CO_2 emission was detected by the non-dispersible infrared absorption (NDIR) to calculate the TC and IC content, separately. The mass fractions of TC and IC were tested separately, and the difference yielded the TOC. Hydrolysis nitrogen was determined by applying the alkaline hydrolysis diffusion method. About 2 g of soil sample that was sieved using 2-mm mesh was evenly paved in the outer chamber of a diffusion dish with 1 g zinc-ferrous sulfate reductant. A 3 mL boric acid indicator was added in the inner chamber of the diffusion dish, and alkaline glue was evenly smeared on the edge of the outer chamber. About 10 mL and 1.8 mol$\cdot$L^{-1} sodium hydroxide solution was injected into the outer chambers and uniformly mixed. The diffusion dishes were sealed and placed in a thermostat with the temperature set under 40 °C. The boric acid indicator in the inner chamber was titrated with standard hydrochloric acid solution after 24 h. pH was measured through the potentiometer method using a pHS-3C pH

meter (Rex China); the water-soil ratio was 5:2. EC was measured through the conductivity method using a DDS-307 conductivity meter (Rex China); the water-soil ratio was 5:1. Each soil sample was replicated thrice.

2.3. Gas Sampling and Testing

Fluxes of CO_2, CH_4, and N_2O were collected using the manual closed chamber technique. The bottom edge of each chamber (50 cm × 50 cm × 100 cm) was embedded into the base (50 cm × 50 cm × 30 cm), which was previously buried 30 cm into the soil with a seal groove. Three bases were randomly equipped in each plot. The sizes of chamber and base were adapted to rice growth. The distilled water was added into the seal groove to seal the chamber when gas sampling. The temperature inside the chamber was recorded by the attached thermometer. Each chamber was equipped with a circulating fan to ensure complete gas mixing. Gas samples were collected every half hour from 9 a.m. to 11 a.m., and all the plots were monitored twice a week. Each gas sample was replicated thrice. Gas samples were drawn from the chambers using a 50 mL airtight syringe with a three-way stopcock into pre-evacuated vacuum bags; these were immediately taken back to the lab of Northeast Institute of Geography and Agroecology, Chinese Academy of Sciences. CO_2, CH_4, and N_2O were determined in 24 h by using the gas chromatography (GC, Agilent 7820A, Santa Clara, CA, USA) method, which was equipped with a flame ionization detector and an electron capture detector. Also, the column, carrier gas, temperature and other parameters were based on the method of Zhang *et al.* [25]. The gas concentrations were quantified with the comparison of peak areas with reference gases. GHG flux was calculated based on the change of GHG concentration in the chamber, which was estimated as the slope of linear regression between concentration and time.

2.4. Calculation and Statistics

The gas emission flux was estimated by the following equation [10]:

$$F = \rho \times (V/A) \times (\Delta c/\Delta t) \times (273/T) \tag{1}$$

where, F is the emission flux of CO_2, CH_4 or N_2O (mg·m^{-2}·h^{-1}), ρ is the gas density of CO_2, CH_4 or N_2O under a standardized state (mg·cm^{-3}), V is the volume of chamber (m^3), A is the area from which the gas is emitted into the chamber (m^2), $\Delta c/\Delta t$ is the change of gas concentration in the chamber (mg·m^{-2}·h^{-1}), and T is the absolute temperature in the chamber.

The gas emission flux of each growing stage is calculated as follows:

$$\overline{F} = \frac{\sum\limits_{i}^{n} F_i}{n} \tag{2}$$

$$\overline{F_{cal}} = C \times \overline{F}$$

where, $\overline{F}$ is the average emission flux of the measured gas (*i.e.*, CO_2, CH_4 and N_2O) from 9 a.m. to 11 a.m. in each growing stage (mg·m^{-2}·h^{-1}), F_i is the measured gas emission flux of collection day in each growing stage (mg·m^{-2}·h^{-1}), n is the number of gas collection days in each growing stage, $\overline{F_{cal}}$ is the calibrated average emission flux of gas (*i.e.*, CO_2, CH_4 and N_2O) during 24 h of one day in each growing stage (mg·m^{-2}·h^{-1}), C is the calibration coefficient which converts the hourly gas emission flux from 9 a.m. to 11 a.m. into that for 24 h of one day. The calibration coefficient is 1.24. It is based on the study of net CO_2 flux of paddy fields with the temperate monsoon climate [26], a climate condition which is similar to that of western Jilin Province. The emission fluxes of CH_4 and N_2O are significantly correlated with that of CO_2, as described below, so the calibration coefficient is also applied for the calculation of CH_4 and N_2O flux.

The cumulative flux of GHG is calculated as follows [10]:

$$F_C = \overline{F_{cal}} \times 24 \times D_i / 1000 \tag{4}$$

where, F_C is the cumulative flux of CO_2, CH_4 or N_2O in each growing stage (g·m^{-2}), D_i is the number of days in the i th growing stage. The green, tillering, booting, heading, and grain filling stages are 17 days, 27 days, 34 days, 26 days, and 36 days, respectively.

The global GWP of main GHGs reported by the IPCC Fourth Assessment Report (2007) are described in Table 2. The global warming potential of CO_2 is 1 and is the reference gas of global warming potential assessment.

Table 2. Global warming potential of CH_4 and N_2O.

Greenhouse Gas	Life Period (year)	The Evaluation Time of Global Warming Potential		
		20 years	100 years	500 years
CH_4	12	72	25	7.6
N_2O	114	289	298	153

The contributions of CH_4 and N_2O to the greenhouse effect are much larger than that of CO_2 by 25 times and 298 times, respectively. The GHG emission flux of CO_2, CH_4, and N_2O produced from paddy fields of different reclamation years during the growing period (CO_2-meter) were calculated using the formula.

$$F_{C_{CO\,2-eqv}} = 25 F_{C_{CH\,4}} + 298 F_{C_{N2O}} + F_{C_{CO\,2}} \tag{5}$$

where, $F_{C_{co2-eqv}}$ is the GHG cumulative flux (CO_2-meter, gCO_2-eqv·m^{-2}), $F_{C_{CH\,4}}$ is the cumulative flux of CH_4 (g·m^{-2}), $F_{C_{N2O}}$ is the cumulative flux of N_2O (g·m^{-2}), and $F_{C_{CO\,2}}$ is the cumulative flux of CO_2 (g·m^{-2}).

3. Results

3.1. Emission Laws of GHG of Paddy Fields in Different Stages of Growing Season

The emission fluxes of CO_2 and CH_4 showed obvious variation laws (Figure 1). The CO_2 emission flux reached the maximum (991.88–1267.17 mg·m^{-2}·h^{-1}) in the tillering stage, then slightly decreased in the booting stage, continued to decline in the heading stage, and finally increased in the grain filling stage. The emission flux of CH_4 showed a single peak (9.76–17.89 mg·m^{-2}·h^{-1}) in the booting stage. The emission flux of N_2O was small, and the range was from 0.026 to 0.047 mg·m^{-2}·h^{-1}. Also, the emission fluxes of N_2O were slightly higher in the tillering, booting and heading stages than that of other stages.

The GHG cumulative flux of rice in different growing stages followed the trend of increasing in the tillering and booting stages, decreasing in the heading stage and increasing in the grain filling stage, which peaked at the booting stage ranging from 837.61 to 1377.83 gCO$_2$-eqv·m^{-2} (Figure 2). The emission contribution rates of CO_2, CH_4, and N_2O differed at different growing stages (Figure 3). The emission contribution rates of CH_4 and N_2O were slight in the green and grain filling stages, and their sum did not exceed 10%. Except for the paddy field developed for one year, the mean contribution rates of CH_4 and N_2O are 4.13% and 3.20% in the green stage, respectively. The contribution rate of CH_4 was two to five times that of N_2O in the grain filling stage. In the tillering, booting, and heading stages, rice rapidly developed, the contribution rate of CO_2 was reduced (85.16%–61.79%), the contribution rate of CH_4 increased significantly (13.78%–36.74%), and the contribution rate of N_2O was maintained at about 1%. CO_2 emissions were dominant in the green and grain filling stages. The emission levels of CH_4 and N_2O were similar as those in the green stage. The contributions to the greenhouse effect of N_2O and CH_4 decreased and increased in the grain filling stage, respectively.

In the tillering, booting and heading stages, the contribution rate of CO_2 emission decreased, while that of CH_4 increased, and the proportion of the former was higher than that of N_2O.
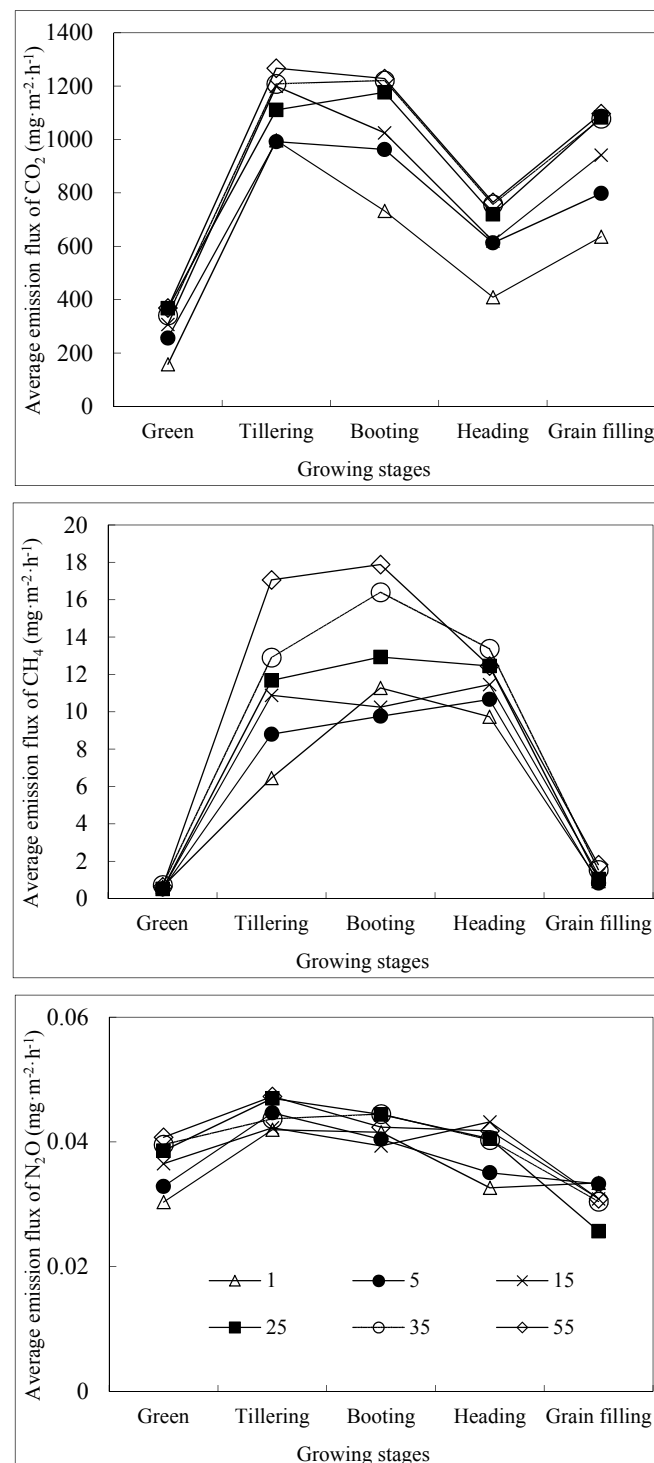

Figure 1. GHG emission fluxes of paddy soil. Note: Legend represents paddy fields of different reclamation periods. e.g., 55 represents the paddy field reclaimed for 55 years.
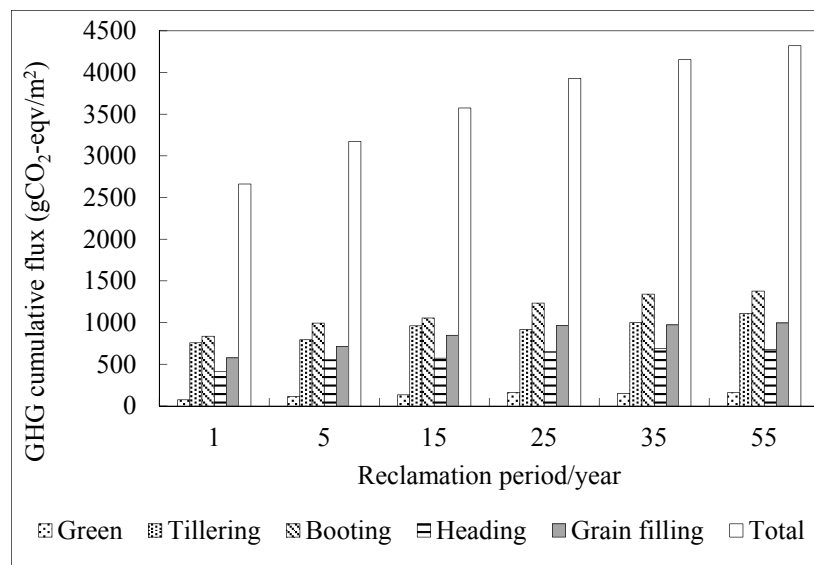
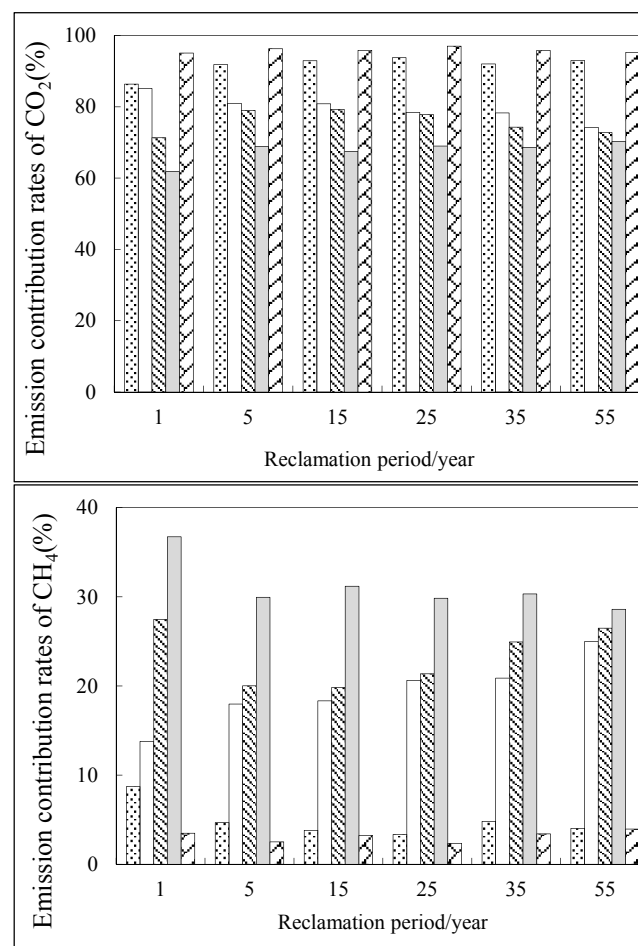**Figure 2.** GHG cumulative fluxes of paddy fields in different growing stages.
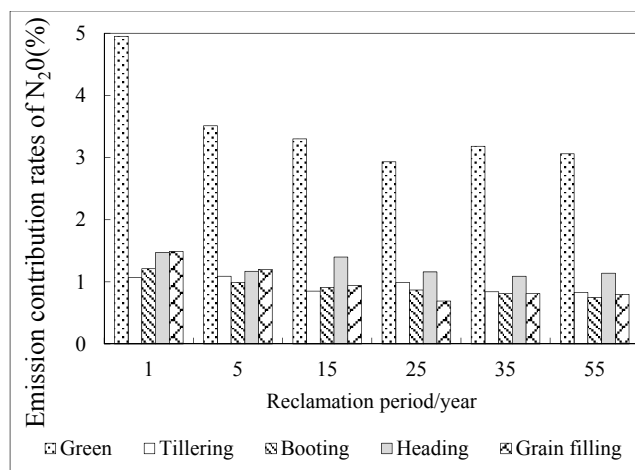

Figure 3. *Cont.*

Figure 3. GHG emission contribution rates of paddy fields in different growing stages.

3.2. GHG Emission Laws of Paddy Fields of Different Reclamation Periods

The emission fluxes of CO_2, CH_4 and N_2O of the paddy field which was reclaimed for one year were lower, while those of the paddy field reclaimed for 55 years were higher (Figure 1). Total cumulative flux of GHG (CO_2-meter) increased with the increasing reclamation period of paddy fields (Figure 2). Except for the paddy field reclaimed for one year, the contribution rate of CH_4 emission was elevated with the lengthening cultivation period (Figure 4). CO_2 emission had an annual average contribution rate of 80.70%. The contribution rates of CH_4 ranged from 16.69% to 20.39% and those of N_2O ranged from 0.93% to 1.37%. The contribution rate of CH_4 was 14–22 times greater than that of N_2O, indicating that the contribution of the CH_4 emission of paddy fields to the regional greenhouse effect cannot be ignored. With the increasing reclamation periods, the contribution rate of CO_2 first increased and then decreased; meanwhile, the contribution rate of CH_4 first decreased then increased and that of N_2O decreased annually.
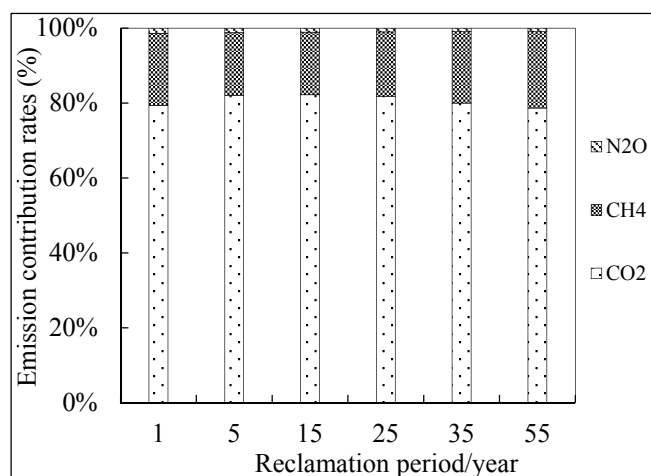

Figure 4. Emission contributions of CO_2, CH_4, and N_2O in different reclamation periods.

Figure 5 showed that the cumulative fluxes of CO_2, CH_4, and N_2O continuously increased with the increasing reclamation periods. The cumulative flux of CO_2 of paddy field reclaimed for 1, 5, 15, 25, 35, 55 years was 2112.73, 2604.29, 2939.22, 3215.17, 3322.92, 3399.52 g·m^{-2}, respectively. That of CH_4 was 20.52, 21.25, 23.87, 27.00, 31.71, 35.25 g·m^{-2}, respectively. That of N_2O was 0.122, 0.126, 0.128, 0.130, 0.132, 0.135 g·m^{-2}, respectively.
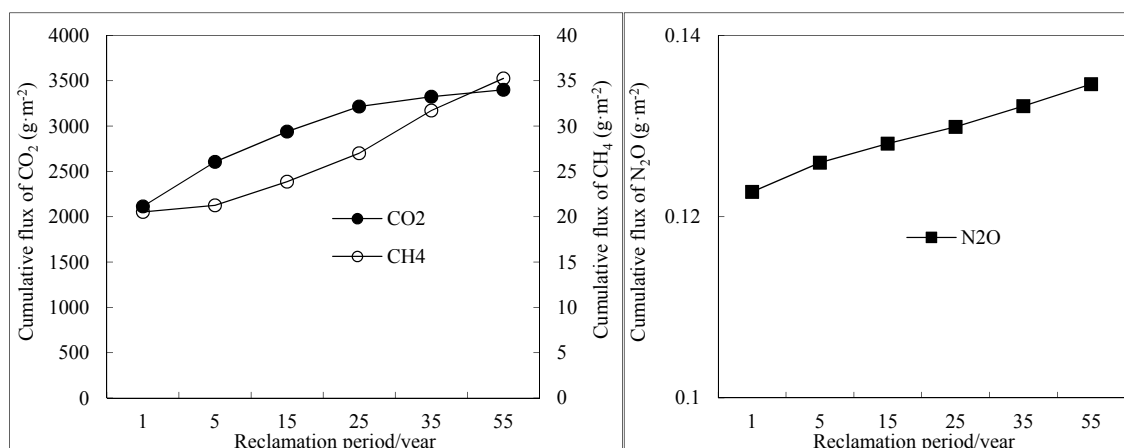
Figure 5. Cumulative fluxes of CO_2, CH_4, and N_2O in different reclamation periods.

3.3. Relationship between GHG Emissions and the Influence Factors

A significant positive correlation was found between the average emission fluxes of CO_2, CH_4, and N_2O, except for the paddy field reclaimed for one year (Table 3). A significant positive correlation was found between the respective average emission fluxes of CO_2, CH_4, and N_2O and the available nitrogen and SOC, whereas a significant negative correlation was observed between the respective average emission fluxes of CO_2, CH_4, and N_2O and pH and electrical conductivity. The variations of pH, electrical conductivity, available nitrogen and SOC were responsible for the GHG emission. A stepwise regression was performed for the emission fluxes of CO_2, CH_4, and N_2O, and regression equations were developed (Table 4).

Table 3. Pearson correlation analysis between seven variables.

	CO_2	CH_4	N_2O	pH	Conductivity	Available Nitrogen	SOC
CO_2	1	0.913 *	0.927 *	−0.959 *	−0.981 **	0.989 **	0.992 **
CH_4		1	0.884 *	−0.934 *	−0.889 *	0.904 *	0.943 *
N_2O			1	−0.918 *	−0.884 *	0.941 *	0.901 *
pH				1	0.892 *	−0.983 **	−0.973 **
Conductivity					1	−0.943 *	−0.968 **
Available nitrogen						1	0.983 **

Note: The average emission fluxes of CO_2, CH_4, and N_2O ($mg \cdot m^{-2} \cdot h^{-1}$) in the growing season of paddy fields of different reclamation periods (except for one year), pH, electrical conductivity ($ms \cdot cm^{-1}$), available nitrogen ($mg \cdot kg^{-1}$) and SOC ($g \cdot kg^{-1}$) of paddy soil of different reclamation periods are the variables. * significant at the <0.05 level; ** significant at the <0.01 level.

Table 4. Stepwise regression analysis of the emission fluxes of CO_2, CH_4, and N_2O.

Equation	R	Significance
CO_2 = 16.671 × SOC + 500.164	0.992	<0.001
CH_4 = 1.188 × SOC + 4.722	0.943	<0.016
N_2O = 0.333 × available nitrogen + 3.292	0.941	<0.017

Note: Y variables are the average emission fluxes of CO_2, CH_4, and N_2O ($mg \cdot m^{-2} \cdot h^{-1}$) in the growing season of paddy fields of different reclamation periods (except for one year), respectively. And X variables are pH, electrical conductivity ($ms \cdot cm^{-1}$), available nitrogen ($mg \cdot kg^{-1}$) and SOC ($g \cdot kg^{-1}$) of paddy soil of different reclamation periods.

4. Discussion

4.1. Emission Laws of GHG of Paddy Fields in Different Stages of the Growing Season

CO_2 emission was significantly impacted by rice growth, and its rate reflected the development of crop growth. CO_2 emissions of the paddy fields stemmed from the respiration of plants and soil [27]. Hence, more mature rice showed lower emission rates. In the tillering stage, the plants grew tall, the leaf area was increased, and respiration was enhanced [16]; thus, the plant released more CO_2. After the booting stage, plant respiration gradually weakened and the photosynthetic rate decreased; CO_2 emission no longer increased. The conversion of the litter produced by rice plant and soil organic matter after draining and sunning the fields gradually enhanced soil respiration in grain filling stage. Without the effect of flooding, CO_2 was stored in the soil before being emitted into the atmosphere.

H_2/CO_2 reduction and acetic acid fermentation were the main channels of CH_4 production in paddy fields. The fermentation of hydrogen-producing acetogenic bacteria and methanogens also played a major role in CH_4 production [28]. N_2O in soil was mainly produced by nitrification and denitrification with the participation of microbes. The metabolic activities of fermented bacteria provided available carbon source for denitrification in the early tillering stage. Paddy fields emitted a large amount of N_2O by the nitrification and denitrification of bacteria. However, CH_4 emission of paddy fields was less because the environmental conditions (*i.e.*, Eh) were not conducive to the growth and reproduction of hydrogen-producing acetogenic bacteria and methanogenic bacteria. In the tillering, booting and heading stages, rice growth was vigorous, and soil microbes were active because of the high temperature [29]. The exudates of rice root provided abundant carbon source and energy for methanogens, whereas the deep water layers of the paddy fields provided a good anaerobic condition for soil. This resulted in the ideal development of the aerenchyma of rice, thus demonstrating that CH_4 emission was at its peak. A substantial increase of the number of microbial flora producing CH_4 led to the massive emission of CH_4 after the rice fields were flooded. However, the anaerobic environment inhibited the activity of nitrifying and methane-oxidizing bacteria, which resulted in less N_2O emission. Drainage facilitated nitrification; thus, N_2O emission appeared at its peak after paddy fields were drained in the booting stage. Fertilization was also the cause of the substantial increase of N_2O emission. Nitrogen fertilizer provided more substrates for microbes, resulted in the increase of N_2O emission in the green, tillering, and booting stages.

GHG emission of paddy soil in different stages of growing season can be attributed to the growth status and soil conditions. The contribution rate of CH_4 increased during the rice flourishing season because of the good anaerobic environment for soil microbes provided by the flooding layer and the developed aerenchymas of the rice plants [30]. In comparison, drainage and dry conditions limited CH_4 emissions [31].

4.2. GHG Emission Laws of Paddy Fields of Different Reclamation Periods

The total amount of GHG emissions increased with the increasing reclamation period of paddy fields. The reason was that SOC had an accumulation trend in the reclamation process of paddy fields [32], providing the substrate for soil microbes metabolism and ultimately affecting GHG emissions. The high pH and salinity in soil inhibited the growth of microbes, and ultimately affected the GHG emission [18,33]. With the reclamation of paddy fields, pH and salinity decreased after large-scale irrigation, thus forming a suitable environment for the growth of microorganisms. So, GHG emissions increased with the increasing reclamation periods. The CH_4 emission flux measured in the saline-alkali paddy fields was lower than that in the transplanting paddy fields without straw incorporation in Jianghuai area [15] and the rice field in the Chaohu low-lying areas, which were normally under the traditional cultivation conditions [22]. Meanwhile, that of N_2O was lower than that in the transplanting paddy fields in Jianghuai area [15] and was equivalent to the rice field in the low-lying areas in Chaohu, except for the peak [22]. This was mostly related to the high degree of

salinization, low organic matter content, small number and activity of microorganisms, and weak soil respiration in the paddy soils in new reclamation areas.

4.3. Influence Factors of GHG Emission

pH of paddy soil gradually decreased with the increasing reclamation years. However, the average emission flux of CO_2 and CH_4 gradually increased, and the N_2O average emission flux of the plots reclaimed for five and 15 years were lower than those of other plots. There was a negative correlation between pH and the emission fluxes of CO_2, CH_4, and N_2O. Li *et al.* [32] found that pH was negatively correlated with CO_2 and N_2O emission flux in different types of alpine grassland. pH also affected the formation and decomposition of soil organic matter and the activity of microorganism and root growth; thus, GHG emissions changed [33]. pH is one of the important factors in the formation processes of CH_4. Methane bacteria can normally grow in a neutral or weak acid environment [34]. The lower pH inhibits methanogen growth [34]. Higher pH enhances CH_4 production when pH ranges from 3 to 7 [35]. The production of CH_4 declines when pH exceeds 8 [36]. The emission capacity of CH_4 almost disappears when pH is less than 5.75 or more than 8.75 [37]. In comparison, the effect of pH on N_2O emission is complex. Soil pH is an important factor affecting both nitrification and denitrification [38]. Low pH may affect both the nitrification and denitrification processes and inhibit the activity of the N_2O reductases responsible for the conversation of N_2O during denitrification, which then leads to increased N_2O emissions [39]. Wang [40] reported that the flux of N_2O from soil to atmosphere decreased as soil pH increased.

As conductivity—the variation of which was in agreement with salinity—was higher in the paddy fields, the average emission fluxes of CO_2, CH_4, and N_2O were lower. Although few studies on the effects of soil salt on GHGs emission of the paddy fields have been carried out, some have reported that soil soluble salt has an impact on the growth of rice and the survival of soil microbes [41]. Furthermore, the morphology and growth of rice determines the rate of photosynthesis, respiration, and transpiration. The interaction occurs between the roots and soil microorganisms. The number and community structure of microorganisms affect the generation and emission of GHGs [42].

When the available nitrogen content was lower in the paddy fields, the emission fluxes of CO_2, CH_4, and N_2O were lower. The positive correlations between soil available nitrogen and the emission fluxes of CO_2, CH_4, and N_2O are consistent with the conclusion of Li *et al.* [32] who reported that CO_2 emission is positively correlated with TN, NO_3^--N, and NH_4^+-N in different types of alpine grasslands. Some studies on the relationship between soil available nitrogen and GHG emission have been carried out. For example, Li *et al.* [32] reported that NO_3^--N is one of the key factors that affect N_2O emissions in May and October of each year. Grandy *et al.* (2008) showed that the increase of available nitrogen in the soil decreases the activity of the oxidase, which inhibit CO_2 emissions. Skiba *et al.* [43] and Smith *et al.* [44] reported the correlation between N_2O emissions and inorganic nitrogen concentration, whereas Oleg and Bernd [45] found that N_2O emissions are negatively correlated with soil total nitrogen and the ratio of carbon to nitrogen.

When the SOC content was lower in the paddy fields, the emission fluxes of CO_2, CH_4, and N_2O were lower. SOC is the main carbon source of soil respiration [21]. At the same time, SOC content has a direct effect on soil microorganism activity which, in turn, affects GHG emission. Chen *et al.* [46] reported the hyperbolic relationship between soil respiration and organic carbon content. Low SOC content limits soil respiration, whereas high SOC content weakens the positive effect on soil respiration. Another study found that the correlation between soil respiration and SOC content was determined by the proportions of the components that decompose in different degrees (labile and recalcitrant) in the soil as well as the stimulating effect of the plant root exudates and litter [47]. Some studies have reported that SOC content was one of the main controlling factors for the CH_4 emissions [32]. A variety of reducing substances which then served as substrates for methanogenesis [6] were produced by the rapid decomposition of SOC in the anoxic environment found in the irrigated paddy fields. The reduced substances subsidies accelerated the decline of the redox potential of paddy fields, improved

the activity of methanogen, contributed to the formation of the aerenchymas of the plants [16], and provided a suitable environment for the production and emission of methane. Finally, the high organic carbon content promoted denitrification, while the ratio of carbon to nitrogen in organic matter also affected the proportion of products [48].

5. Conclusions

For the paddy soil in a saline-alkali region in western Jilin Province, the seasonal variation of GHG followed the trend of increasing, decreasing and then finally increasing through the entire growing period and peaked at the booting stage. GHG emission of paddy fields reclaimed for different amounts of time decreased in the sequence of booting, tillering, grain filling, heading, and greening stages. GHG emissions were predominantly controlled by CO_2 emissions. The emission flux of CO_2 was observed two peaks in tillering and booting stages and grain filling stage, respectively, and that of CH_4 was found to demonstrate a single peak in the booting stage. The total amount of GHG emissions and the components of the fluxes of CO_2, CH_4, and N_2O increased with the increasing reclamation period. GHG emission was affected by a combination of various factors. A positive correlation was found between the emission fluxes of CO_2, CH_4, and N_2O and available nitrogen and SOC. A negative correlation was observed between the emission fluxes of CO_2, CH_4, and N_2O and soil pH and conductivity. Our results were applicable for the assessment of regional GHG emissions in different reclamation periods of the paddy soil.

Author Contributions: Jie Tang and Zhaoyang Li designed the research; Shuang Liang and Hao Zhang collected and tested the samples; Nan Zhang and Sining Wang analyzed the data; Shuang Liang drafted the manuscript which was revised by Jie Tang. Shuang Liang and Hao Zhang modified the paper. All authors have read and approved the final manuscript.

Conflicts of Interest: The authors declare no conflict of interest.

References

1. Solomon, S.; Qin, D.; Manning, M.; Chen, Z.; Marquis, M.; Averyt, K.B.; Tignor, M.; Miller, H.L. *Climate Change 2007: The Physical Science Basis, Contribution of Working Group I to the Fourth Assessment Report of the Intergovernmental Panel on Climate Change*, 1st ed.; Cambridge University Press: Cambridge, UK; New York, NY, USA, 2007; pp. 2–18.

2. Bhattacharyya, P.; Neogi, S.; Roy, K.S.; Dash, P.K.; Nayak, A.K.; Mohapatra, T. Tropical low land rice ecosystem is a net carbon sink. *Agric. Ecosyst. Environ.* **2014**, *189*, 127–135. [CrossRef]

3. Zhao, Y.N.; Zhang, Y.Q.; Du, H.X.; Wang, Y.H.; Zhang, L.M.; Shi, X.J. Carbon sequestration and soil microbes in purple soil as affected by long-term fertilization. *Toxicol. Environ. Chem.* **2015**, *97*, 464–476. [CrossRef]

4. Farooq, M.; Kadambot, H.M.; Rehman, H.; Aziz, T.; Lee, D.-J.; Wahid, A. Rice direct seeding: Experiences, Challenges and Opportunities. *Soil Tillage Res.* **2011**, *111*, 87–98. [CrossRef]

5. Bhattacharyya, P.; Nayak, A.K.; Mohanty, S.; Tripathia, R.; Shahida, M.; Kumara, A.; Rajaa, R.; Pandaa, B.B.; Roya, K.S.; Neogia, S.; *et al.* Greenhouse gas emission in relation to labile soil C, N pools and functionalmicrobial diversity as influenced by 39 years long-term fertilizer management intropical rice. *Soil Tillage Res.* **2013**, *129*, 93–105. [CrossRef]

6. Yao, H.; Conrad, R. Electron balance during steady-state production of CH_4 and CO_2 in anoxic rice soil. *Eur. J. Soil Sci.* **2000**, *51*, 369–378. [CrossRef]

7. Szafranek-Nakonieczna, A.; Stêpniewska, Z. Erobic and anaerobic respiration in profiles of Polesie Lubelskie peatlands. *Int. Agrophys.* **2014**, *28*, 219–229. [CrossRef]

8. He, G.X.; Li, K.H.; Liu, X.J.; Gong, Y.M.; Hu, Y.K. Fluxes of methane, carbon dioxide and nitrous oxide in an alpine wetland and an alpine grassland of the Tianshan Mountains, China. *J. Arid Land* **2014**, *6*, 717–724. [CrossRef]

9. Tang, X.L.; Liu, S.G.; Zhou, G.Y.; Zhang, D.Q.; Zhou, C.Y. Soil-atmospheric exchange of CO_2, CH_4, and N_2O in three subtropical forest ecosystems in southern China. *Glob. Change Biol.* **2006**, *12*, 546–560. [CrossRef]

10. Haque, M.M.; Kim, S.Y.; Ali, M.A.; Kim, P.J. Contribution of greenhouse gas emissions during cropping and fallow seasons on total global warming potential in mono-rice paddy soils. *Plant Soil* **2015**, *387*, 251–264. [CrossRef]

11. Phillips, R.L.; Tanaka, D.L.; Archer, D.W.; Hanson, J.D. Fertilizer application timing influences greenhouse gas fluxes over a growing season. *J. Environ. Qual.* **2009**, *38*, 1569–1579. [CrossRef] [PubMed]

12. Rafique, R.; Kumar, S.; Luo, Y.Q.; Xu, X.L.; Li, D.J.; Zhang, W.; Asam, Z.-U.-Z. Estimation of greenhouse gases (N_2O, CH_4 and CO_2) fromno-till cropland under increased temperature and altered precipitation regime: A DAYCENT Model Approach. *Glob. Planet. Change* **2014**, *118*, 106–114. [CrossRef]

13. Adviento-Borbe, M.A.; Padilla, G.N.; Pittelkow, C.M.; Simmonds, M.; van Kessel, C.; Linquist, B. Methane and nitrous oxide emissions from flooded rice systems following the end-of-season drain. *J. Environ. Qual.* **2015**, *44*, 1071–1079. [CrossRef] [PubMed]

14. Wang, M.X.; Shangguan, X.J. CH_4 emission from various rice fields in P.R. China. *Theor. Appl. Climatol.* **1996**, *55*, 129–138. [CrossRef]

15. Hang, X.N.; Zhang, X.; Song, C.l.; Jiang, Y.; Deng, A.X.; He, R.Y.; Lu, M.; Zhang, W.J. Differences in rice yield and CH_4 and N_2O emissions among mechanical planting methods with straw incorporation in Jianghuai area, China. *Soil Tillage Res.* **2014**, *144*, 205–210. [CrossRef]

16. Chen, W.W.; Wang, Y.Y.; Zhao, Z.C.; Cui, F.; Gu, J.X.; Zheng, X.H. The effect of planting density on carbon dioxide, methane and nitrous oxide emissions from a cold paddy field in the Sanjiang Plain, northeast China. *Agric. Ecosyst. Environ.* **2013**, *178*, 64–70. [CrossRef]

17. Qin, Y.M.; Liu, S.W.; Guo, Y.Q.; Liu, Q.H.; Zou, J.W. Methane and nitrous oxide emissions from organic and conventionalrice cropping systems in Southeast China. *Biol. Fertil. Soils* **2010**, *46*, 825–834. [CrossRef]

18. Luo, W.H.; Phan, H.V.; Hai, F.I.; Price, W.E.; Guo, W.S.; Ngo, H.H.; Yamamoto, K.; Nghiem, L.D. Effects of salinity build-up on the performance and bacterial community structure of a membrane bioreactor. *Bioresour. Technol.* **2015**, *200*, 305–310. [CrossRef] [PubMed]

19. Zhang, G.X.; Deng, C.N. Gas exchange and chlorophyll fluorescence of salinity-alkalinity stressed Phragmites australis seedlings. *J. Food Agric. Environ.* **2012**, *10*, 880–884.

20. Wang, J.S.; Zhao, C.Y.; Wang, Y.; Zhou, X.Y.; Cui, Y.; Zhang, Y.S.; Sun, F.H.; Wang, X.Y.; Chen, P.S.; Liu, Y.Y.; *et al.* *Summary of Decision Makers and Executive Summary of Climate Change Assessment Report in the Northeast Region*, 1st ed.; China Meteorological Press: Beijing, China, 2013; pp. 4–8.

21. Watanabe, A.; Machida, N.; Takahashi, K.; Kitamura, S.; Kimura, M. Flow of photosynthesized carbon from rice plants into the paddy soil ecosystem at different stages of rice growth. *Plant Soil* **2004**, *258*, 151–160. [CrossRef]

22. Jiang, B.; Yang, S.Y.; Yang, X.B.; Ma, Y.H.; Chen, X.L.; Zuo, H.F.; Fan, D.F.; Gao, L.; Yu, Q.; Yang, W. Effect of controlled drainage in the wheat season on soil CH_4 and N_2O emissions during the rice season. *Int. J. Plant Product.* **2015**, *9*, 273–291.

23. Li, Y.Y.; Dong, S.K.; Liu, S.L.; Zhou, H.K.; Gao, Q.Z.; Cao, G.M.; Wang, X.X.; Su, X.K.; Zhang, Y.; Tang, L.; *et al.* Seasonal changes of CO2, CH4 and N2O fluxes in different types of alpine grassland in the Qinghai-Tibetan Plateau of China. *Soil Biol. Biochem.* **2015**, *80*, 306–314. [CrossRef]

24. Moiwo, J.P.; Lu, W.X.; Zhao, Y.S.; Yang, Y.H.; Yang, Y.M. Impact of land use on distributed hydrological processesin the semi-arid wetland ecosystem of Western Jilin. *Hydrol. Proc.* **2010**, *24*, 492–503.

25. Zhang, J.B.; Song, C.C.; Yang, W.Y. Cold season CH_4, CO_2 and N_2O fluxes from freshwater marshes in northeast China. *Chemosphere* **2005**, *59*, 1703–1705. [CrossRef] [PubMed]

26. Nishimura, S.; Yonemura, S.; Minamikawa, K.; Yagi, K. Seasonal and diurnal variations in net carbon dioxide flux throughout the year from soil in paddy field. *J. Geophys. Res. Biogeosci.* **2015**, *120*, 63–76. [CrossRef]

27. Lou, Y.S.; Ren, L.X.; Li, Z.P.; Zhang, T.L.; Inubushi, K. Effect of rice residues on carbon dioxide and nitrous oxide emissions from a paddy soil of subtropical China. *Water Air Soil Pollut.* **2007**, *178*, 157–168. [CrossRef]

28. Liesack, W.; Schnell, S.; Revsbech, N.P. Microbiology of flooded rice paddies. *FEMS Microbiol. Rev.* **2000**, *24*, 625–645. [CrossRef] [PubMed]

29. Wu, Y.P.; Yu, X.S.; Wang, H.Z.; Ding, N.; Xu, J.M. Does history matter? Temperature effects on soil microbial biomass and community structure based on the phospholipid fatty acid (PLFA) analysis. *J. Soils Sediments* **2010**, *10*, 223–230. [CrossRef]

30. Nouchi, I.; Hosono, T.; Aoki, K.; Minami, K. Seasonal variation in methane flux from rice paddies associated with methane concentration in soil water, rice biomass and temperature, and its modelling. *Plant Soil* **1994**, *161*, 195–208. [CrossRef]

31. Pandey, A.; Mai, V.T.; Vu, D.Q.; Bui, T.P.L.; Mai, T.L.A.; Jensen, L.S.; de Neergaard, A. Organic matter and water management strategies to reduce methane and nitrous oxide emissions from rice paddies in Vietnam. *Agric. Ecosyst. Environ.* **2014**, *196*, 137–146.

32. Olsson, L.; Ye, S.; Yu, X.; Wei, M.; Krauss, K.W.; Brix, H. Factors influencing CO_2 and CH4 emissions from coastal wetlands in the Liaohe Delta, Northeast China. *Biogeosciences* **2015**, *12*, 4965–4977. [CrossRef]

33. Parmar, K.; Keith, A.M.; Rebecca, L.R.; Sohi, S.P.; Moeckel, C.; Pereira, M.G.; McNamara, N.P. Bioenergy driven land use change impacts on soil greenhouse gas regulation under Short Rotation Forestry. *Biomass Bioenergy* **2015**, *82*, 40–48. [CrossRef]

34. Treat, C.; Natali, S.; Ernakovich, J.; Iversen, C.M.; Lupascu, M.; McGuire, A.D.; Norby, R.J.; Roy Chowdhury, T.; Richter, A.; Šantrůčková, H.; *et al*. A pan-Arctic synthesis of CH_4 and CO_2 production from anoxic soil incubations. *Glob. Change Biol.* **2015**, *21*, 2787–2803. [CrossRef] [PubMed]

35. Ye, R.; Jin, Q.; Bohannan, B.; Keller, J.K.; McAllister, S.A.; Bridgham, S.D. pH controls over anaerobic carbon mineralization, the efficiency of methane production, and methanogenic pathways in peatlands across an ombrotrophic-minerotrophic gradient. *Soil Biol. Biochem.* **2012**, *54*, 36–47. [CrossRef]

36. Leu, J.Y.; Lin, Y.H.; Chang, F.L. Conversion of CO2 into CH4 by methane-producing bacterium FJ10 under a pressurized condition. *Chem. Eng. Res. Des.* **2011**, *89*, 1879–1890. [CrossRef]

37. Chaum, S.; Supaibulwattana, K.; Kirdmanee, C. Comparative effects of salt stress and extreme pH stress combined on glycinebetaine accumulation, photosynthetic abilities and growth characters of two rice genotypes. *Rice Sci.* **2009**, *16*, 274–282. [CrossRef]

38. Khan, S.; Clough, T.J.; Goh, K.M.; Sherlock, R.R. Influence of soil pH on NOx and N_2O emissions from bovine urine applied to soil. *N. Z. J. Agric. Res.* **2011**, *54*, 285–301. [CrossRef]

39. Audet, J.; Hoffmann, C.C.; Andersen, P.M.; Baattrup-Pedersen, A.; Johansen, J.R.; Larsen, S.E.; Kjaergaard, C.; Elsgaard, L. Nitrous oxide fluxes in undisturbed riparian wetlands located in agricultural catchments: Emission, Uptake and Controlling Factors. *Soil Biol. Biochem.* **2014**, *68*, 291–299. [CrossRef]

40. Wang, B.; Lee, X.Q.; Theng, B.; Cheng, J.; Yang, F. Diurnal and spatial variations of soil NOx fluxes in the northern steppe of China. *J. Environ. Sci.* **2015**, *32*, 54–61. [CrossRef] [PubMed]

41. Hasbullah, H.; Marschner, P. Residue properties influence the impact of salinity on soil respiration. *Biol. Fertil. Soils* **2015**, *51*, 99–111. [CrossRef]

42. Farías, L.; Florez-Leiva, L.; Besoain, V.; Sarthou, G.; Fernández, C. Dissolved greenhouse gases (nitrous oxide and methane) associated with the naturally iron-fertilized Kerguelen region (KEOPS 2 cruise) in the Southern Ocean. *Biogeosciences* **2015**, *12*, 1925–1940. [CrossRef]

43. Skiba, U.M.; Sheppard, L.J.; Macdonald, J.; Fowler, D. Some key environmental variables controlling nitrous oxide emissions from agricultural and semi-natural soils in Scotland. *Atmos. Environ.* **1998**, *32*, 3311–3320. [CrossRef]

44. Smith, K.A.; McTggart, I.P.; Dobbie, K.E.; Conen, F. Emissions of N_2O from Scottish agricultural soils, as a function of fertilizer N. *Nutr. Cycl. Agroecosyst.* **1998**, *5*, 123–130. [CrossRef]

45. Oleg, V.M.; Bernd, H. Activity of denitrification and dynamics of N_2O release in soils under six tree species and grassland in central Siberia. *J. Plant Nutr. Soil Sci.* **1999**, *162*, 533–538.

46. Chen, S.T.; Huang, Y.; Zou, J.W. Modeling interannual variability of global soil respiration from climate and soil properties. *Agric. Forest Meteorol.* **2010**, *150*, 590–605. [CrossRef]

47. Reichstein, M.; Rey, A.; Freibauer, A.; Tenhunen, J.; Valentini, R.; Banza, J.; Casals, P.; Cheng, Y.F.; Grünzweig, J.M.; Irvine, J.; *et al*. Modeling temporal and large-scale spatial variability of soil respiration from soil water availability, temperature and vegetation productivity indices. *Glob. Biogeochem. Cycles* **2003**, *17*, 1029–2035. [CrossRef]

48. Guo, J.P.; Zhou, C.D. Greenhouse gas emissions and mitigation measures in Chinese agroecosystems. *Agric. Forest Meteorol.* **2007**, *142*, 270–277. [CrossRef]